Report

A PHABULOSA/Cytokinin Feedback Loop Controls Root Growth in *Arabidopsis*

Raffaele Dello Ioio,[1] Carla Galinha,[1] Alexander G. Fletcher,[2] Stephen P. Grigg,[1,7] Attila Molnar,[3] Viola Willemsen,[4] Ben Scheres,[4] Sabrina Sabatini,[5] David Baulcombe,[3] Philip K. Maini,[2] and Miltos Tsiantis[1,6,*]

[1]Department of Plant Sciences, University of Oxford, Oxford OX1 3RB, UK
[2]Centre for Mathematical Biology, Mathematical Institute, University of Oxford, Oxford OX1 3LB, UK
[3]Department of Plant Sciences, University of Cambridge, Downing Street, Cambridge CB2 3EA, UK
[4]Molecular Genetics, Department of Biology, Faculty of Science, Utrecht University, Padualaan 8, 3584 CH Utrecht, The Netherlands
[5]Laboratory of Functional Genomics and Proteomics of Model Systems, Dipartimento di Biologia e Biotecnologie, Sapienza Università di Roma, Via dei Sardi 70, 00185 Rome, Italy
[6]Max Planck Institute for Plant Breeding Research, Carl-von-Linne-Weg 10, D-50829 Cologne, Germany

Summary

The hormone cytokinin (CK) controls root length in *Arabidopsis thaliana* by defining where dividing cells, derived from stem cells of the root meristem, start to differentiate [1–6]. However, the regulatory inputs directing CK to promote differentiation remain poorly understood. Here, we show that the HD-ZIPIII transcription factor PHABULOSA (PHB) directly activates the CK biosynthesis gene *ISOPENTENYL TRANSFERASE 7* (*IPT7*), thus promoting cell differentiation and regulating root length. We further demonstrate that CK feeds back to repress both *PHB* and *microRNA165*, a negative regulator of *PHB*. These interactions comprise an incoherent regulatory loop in which CK represses both its activator and a repressor of its activator. We propose that this regulatory circuit determines the balance of cell division and differentiation during root development and may provide robustness against CK fluctuations.

Results and Discussion

How the balance between stem cell activity, cell proliferation, and cell differentiation influences organ size and development is a central question in biology. The *Arabidopsis thaliana* root meristem is an excellent system in which to study this question because it shows a clear differentiation gradient along its proximal-distal axis (Figure 1A). The stem cell niche (STN) resides distally at the root tip and harbors stem cells that give rise to the entire root. More proximally in the division zone (DZ), proliferating cells divide symmetrically, akin to transit amplifying cells in animals, and then enter the elongation/differentiation zone (EDZ), where they cease dividing and grow by elongation. The boundary between the division and differentiation zones is called the transition zone (TZ), and its positioning determines the length of the meristem and consequently the root length [1, 2]. The balance between dividing and differentiating cells tends toward a steady state that depends on the regulated interplay of the hormones cytokinin (CK) and auxin [1–6]. An auxin maximum at the root tip promotes stem cell function while an auxin gradient along the meristem fuels cell proliferation in the division zone [3, 4]. CK acts proximally to repress auxin signaling, thus promoting differentiation and defining the position of the TZ [1, 5, 6]. Increased CK shifts the position of the TZ distally, shortening meristem and root length, whereas decreased CK shifts the TZ proximally, producing a longer meristem and root. Despite this key role for CK in controlling root meristem size, little is known about how its regulated activity determines the balance of cell division and differentiation during root growth.

HD-ZIPIII transcription factors are involved in patterning processes throughout plant development [7–14], but the downstream components via which they exert these effects are largely unknown [15]. We suspected that HD-ZIPIIIs might be key components of CK-mediated differentiation pathways because we observed a striking congruence in the mutant phenotypes resulting from perturbed CK and HD-ZIPIII activities. Specifically, we found that microRNA (miRNA)-insensitive *HD-ZIPIII* gain-of-function mutants in which expression of the redundantly acting *PHABULOSA* and *PHAVOLUTA* is increased and broadened (*phb-1d* and *phv-1d*) [7–14] display short roots and small root meristems, reminiscent of the phenotypes observed upon treatment with CK [1] or overexpression of the bacterial CK biosynthesis gene *ISOPENTENYL TRANSFERASE* (*IPT*) (Figures 1B–1G). Similar phenotypes were observed in transgenic lines that broadly expressed a dexamethasone (DEX)-inducible *PHB* version (*PHB**), which is insensitive to miRNA-dependent posttranscriptional repression, using a two-component transactivation system (*35S: LhGR>>PHB**) [16] (see Figures S1A–S1E available online). These findings indicated that PHB and PHV may control the position of the TZ and thus root meristem size in a fashion similar to CK. Two lines of evidence suggested that PHB activity in eliciting such gain-of-function phenotypes is mediated through the CK pathway. First, the expression of the primary response CK target *ARABIDOPSIS RESPONSE REGULATOR 5* (*ARR5*) [17] and the CK activity reporter *TWO-COMPONENT-OUTPUT-SENSOR* green fluorescent protein (*TCS::GFP*) [18] was broadened in *phb-1d/+* and *phv-1d/+* backgrounds (Figures 1C–1E and data not shown). Second, a loss-of-function mutation in *ARR1*, encoding a CK-dependent transcriptional regulator of meristem size [1, 5, 6], was sufficient to suppress the short-root defects of *phb-1d/+* (Figures S1F–S1K). Notably, *ARR1* expression is first detectable 5 days after germination (DAG) when TZ positioning is established and coincides with the time at which *arr1* suppression of *phb-1d/+* is first noticeable (Figure S1K). These observations indicate that perturbation of ARR1-dependent CK signaling underlies *phb-1d/+* root meristem defects. Expression of stem cell and cell proliferation markers was indistinguishable in *phb-1d/+*, *phv-1d/+*, and wild-type (WT) backgrounds (data not shown), indicating that short-root

[7]Present address: Molecular Genetics, Department of Biology, Faculty of Science, Utrecht University, Padualaan 8, 3584 CH Utrecht, The Netherlands
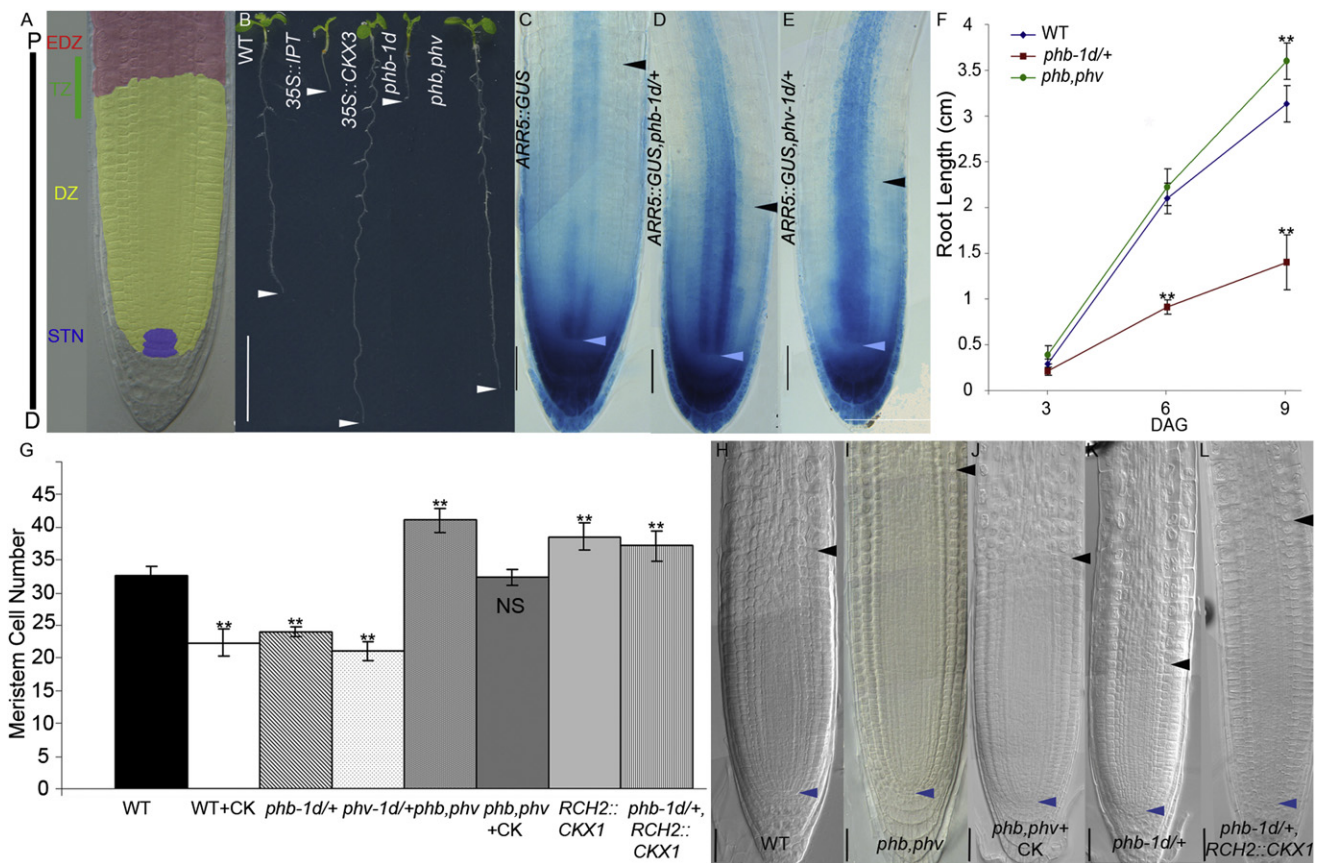*Correspondence: miltos.tsiantis@plants.ox.ac.uk

Figure 1. PHB and PHV Regulate Root Meristem Size through Cytokinin Activity

(A) Organization of the root meristem along the proximal-distal (P-D) axis, showing the stem cell niche (STN, blue), the division zone (DZ, yellow), and the elongation/differentiation zone (EDZ, red). The green line represents the transition zone (TZ).

(B) Ten days after germination (10-DAG) wild-type (WT), *35S::IPT*, *35S::CKX3*, *phb-1d*, and *phb-13,phv-11* plants. White arrowheads point to the root tip. Scale bar represents 1 cm.

(C–E) *ARR5::GUS* in 5-DAG WT (C), *phb-1d/+* (D), and *phv-1d/+* (E) root meristems. Note that *phb-1d/+* and *phv-1d/+* roots have a shorter meristem and stronger *ARR5::GUS* expression in the vasculature than WT. Blue and black arrowheads indicate the stem cell and the TZ of the cortex, respectively. Scale bars represent 50 μm.

(F) Root length measurements over time of WT, *phb-1d/+*, and *phb-13,phv-11* seedlings. Error bars represent SD.

(G) 5-DAG root meristem length in WT, WT treated with cytokinin (CK, 16 hr, 1 μM *trans*-zeatin), *phb-1d/+*, *phv-1d/+*, *phb-13,phv-11*, *phb-13,phv-11* treated with CK, *RCH2::CKX1*, and *RCH2::CKX1,phb-1d/+*. The long-meristem defect of *phb,phv* is rescued by CK treatment, and the short-meristem defect of *phb-1d/+* is rescued by CK depletion at the TZ. Root meristem length was defined as the number of cortex cells between the cortex stem cell (blue arrowhead) and the first elongated cortex cell (black arrowhead). Error bars represent SD.

(H–L) 5-DAG root meristems of WT (H), *phb-13,phv-11* (I), *phb-13,phv-11* treated with CK (1 μM *trans*-zeatin) for 16 hr (J), *phb-1d/+* (K), and *phb-1d/+,RCH2::CKX1* (L). Meristem borders are depicted as in (C–E). Scale bars represent 50 μm.

$*p < 0.05$, $**p < 0.01$, NS, not significant; Student's t test. See also Figure S1.

phenotypes of these mutants are unlikely to reflect stem cell defects but predominantly reflect aberrant TZ positioning. In summary, increased and broadened expression of PHB and PHV is sufficient to cause short roots because of superactivation of CK-dependent cell differentiation pathways.

To determine whether PHB and PHV are also necessary to determine root meristem size, we studied *phb,phv* double mutants, and we observed that they displayed longer roots and longer root meristems than the WT, similar to mutants defective in synthesis or perception of CK (Figures 1B and 1F–1I) [1]. To assess whether PHB and PHV determine root meristem size through influencing CK levels, we treated *phb,phv* seedlings with exogenous CK. A 16 hr CK treatment restored the root phenotype of *phb,phv* to WT (Figures 1G–1J), suggesting that these HD-ZIPIIIs may promote CK biosynthesis. Consistent with these findings, reduction of

CK in *35S:LhGR>>PHB** plants by overexpressing the CK catabolism gene *CKX3* (*35S::CKX3*) restored meristem size and root length (Figures S1A–S1E). Furthermore, overexpression of the CK catabolism gene *CKX1* in the TZ driven by the *ROOT CLAVATA HOMOLOGOUS 2* (*RCH2*) promoter (*RCH2::CKX1*) was sufficient to restore meristem size in *phb-1d/+* mutants (Figures 1G, 1K, and 1L). These observations suggest that the shortened root meristem size and root length in *phd-1d/+* reflects increased CK activity and that PHB may control root meristem size by promoting CK biosynthesis.

CK biosynthesis requires the activity of rate-limiting IPTs [19]. Triple loss-of-function mutants of *IPT3*, *IPT5*, and *IPT7* (*ipt3*, *ipt5*, and *ipt7*) show root meristem defects [1] similar to *phb,phv* plants. On this basis, we hypothesized that PHB and PHV may influence CK activity by activating expression of one or more of these *IPT* genes. Consistent with this
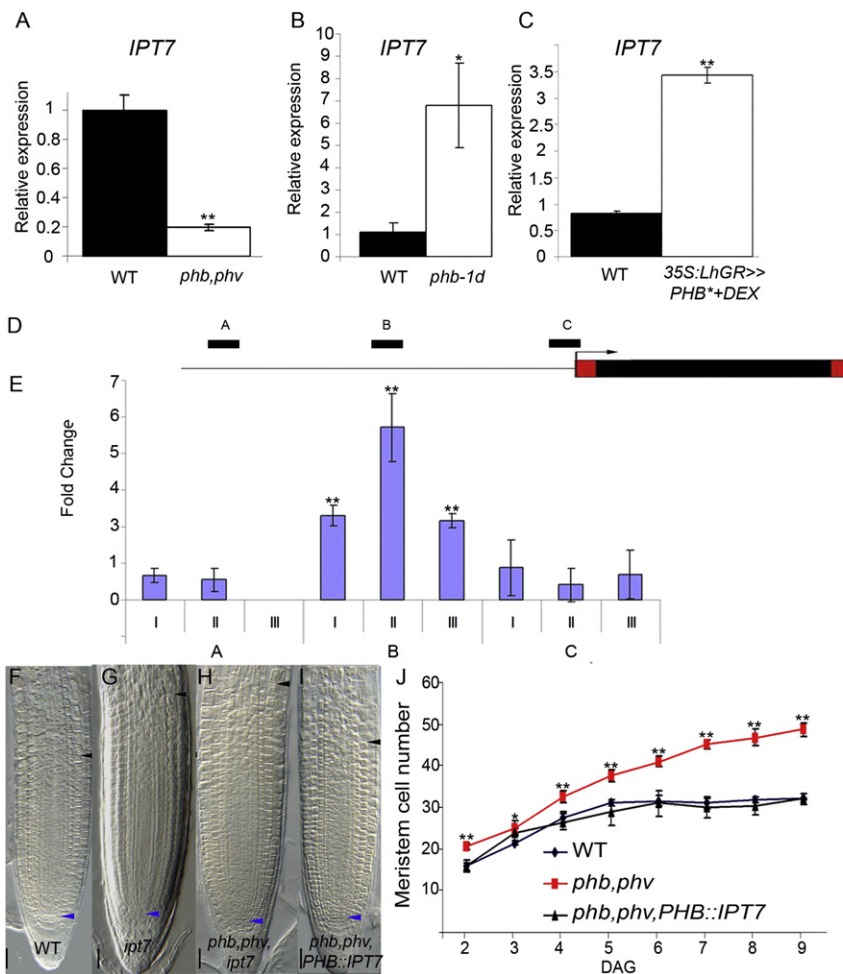
Figure 2. PHB Directly Activates *IPT7*

(A–C) Relative expression of *IPT7* mRNA in *phb-13,phv-11* (A), *phb-1d* (B), and *35S:LhGR>>PHB** plants after 4 hr in 50 μM dexamethasone (DEX) (C). Levels of *IPT7* are strongly reduced in *phb,phv* and strongly enhanced in *phb-1d*. Error bars represent SD; n = 3.

(D) Schematic representation of the *IPT7* gene. The thin line corresponds to the promoter, the red boxes correspond to the untranslated regions, and the black box corresponds to the coding region. The bent arrow represents the transcription start site. A, B, and C correspond to the DNA fragments assayed by ChIP (E).

(E) ChIP analysis. Chromatin from *PHB*:GFP* plants was immunoprecipitated with anti-GFP antibody. The fold enrichment of each DNA fragment (fragments A, B, and C) in relation to the total chromatin input is shown for three independent chromatin extractions (roman numerals). Fragment B is overrepresented in all independent experiments. Error bars represent SD; n = 3.

(F–I) 5-DAG root meristems of WT (F), *ipt7-1* (G), *phb-13,phv-11,ipt7-1* (H), and *phb-13,phv-11,PHB::IPT7* (I). Blue and black arrowheads indicate stem cell and TZ of the cortex, respectively. Scale bars represent 50 μm.

(J) Root meristem cell number of WT, *phb-13,phv-11*, and *phb-13,phv-11,PHB::IPT7* measured over time. *phb,phv* plants do not reach the plateau phase at 5 DAG and continue accumulating cells in the meristem, while in *phb,phv,PHB::IPT7* plants, the plateau phase is reestablished by expressing *IPT7* in the *PHB* domain. Error bars represent SD; n = 40.

*p < 0.05, **p < 0.01; Student's t test. See also Figure S2.

hypothesis, mRNA levels of *IPT7*, but not *IPT3* or *IPT5*, were reduced in *phb,phv* double mutants (Figures 2A, S2A, and S2B) and were increased in *phb-1d* and *phv-1d* mutants and after 4 hr of DEX-induced PHB* expression (Figures 2B, 2C, S2C, and S2D). Thus, PHB is both necessary, through its redundant action with PHV, and sufficient for activation of *IPT7* expression. These observations, together with findings that *PHB* and *IPT7* are expressed in overlapping domains during development (Figures S2E–S2H) [12–20], suggest that PHB and PHV control CK biosynthesis through the activation of *IPT7*. To investigate whether PHB regulates *IPT7* expression by physically interacting with *IPT7* transcriptional complexes, we performed chromatin immunoprecipitation (ChIP) using seedlings expressing a miRNA-insensitive version of *PHB* fused to *GFP* and driven by the *PHB* promoter (*PHB*:GFP*). One fragment of the *IPT7* promoter was overrepresented in the immunoprecipitated chromatin, indicating direct binding to PHB*:GFP (Figures 2D and 2E), which together with the rapid activation of *IPT7* expression upon PHB* induction indicates that *IPT7* is a direct target of PHB.

We next investigated the precise functional significance of PHB-mediated *IPT7* activation for PHB function and root development. We observed that *ipt7-1* and *ipt7-2* single mutants displayed a longer root and root meristem than WT (Figures 2F, 2G, S2I, and S2J), indicating that *IPT7*-dependent CK biosynthesis is sufficient to determine root meristem size. These observations raised a key question: Is IPT7 a central

mediator of PHB/PHV activity in the root meristem, or are additional target genes strictly required for PHB/PHV to promote differentiation? To distinguish between these possibilities, we expressed *IPT7* under the control of *PHB* promoter (*PHB::IPT7*) in a *phb,phv* mutant background. We observed that *PHB::IPT7,phb,phv* plants had WT *IPT7* mRNA abundance and displayed WT root length and meristem size (Figures 2F, 2I, 2J, and S2J–S2L), indicating that IPT7 activity in the *PHB* expression domain fully bypasses the requirement of PHB/PHV for normal root development. Furthermore, the root meristem size of *phb,phv,ipt7* triple mutants was indistinguishable from that of *phb,phv* or *ipt7* mutants (Figures 2H and S2I), confirming that PHB and PHV provide a key developmental input for directing IPT7-dependent differentiation at the TZ. Although these observations highlight the key role of IPT7 in mediating PHB/PHV action, they do not rule out the possibility that PHB/PHV may regulate additional IPT genes. For example, *IPT1* and *PHB* expression domains also overlap in both embryonic and postembryonic roots (Figure S2M) [10, 20, 21], and *IPT1* expression depends on PHB/PHV (Figures S2N and S2O), indicating that IPT1 may also contribute to PHB/PHV-dependent CK activity. Our results provide a striking example of how the expression of a single target gene (*IPT7*) of a developmentally important transcription factor (PHB) can be sufficient to mediate the activity of this transcription factor.

CK action in promoting cell differentiation is self-limiting because above a certain threshold, CK activity represses its
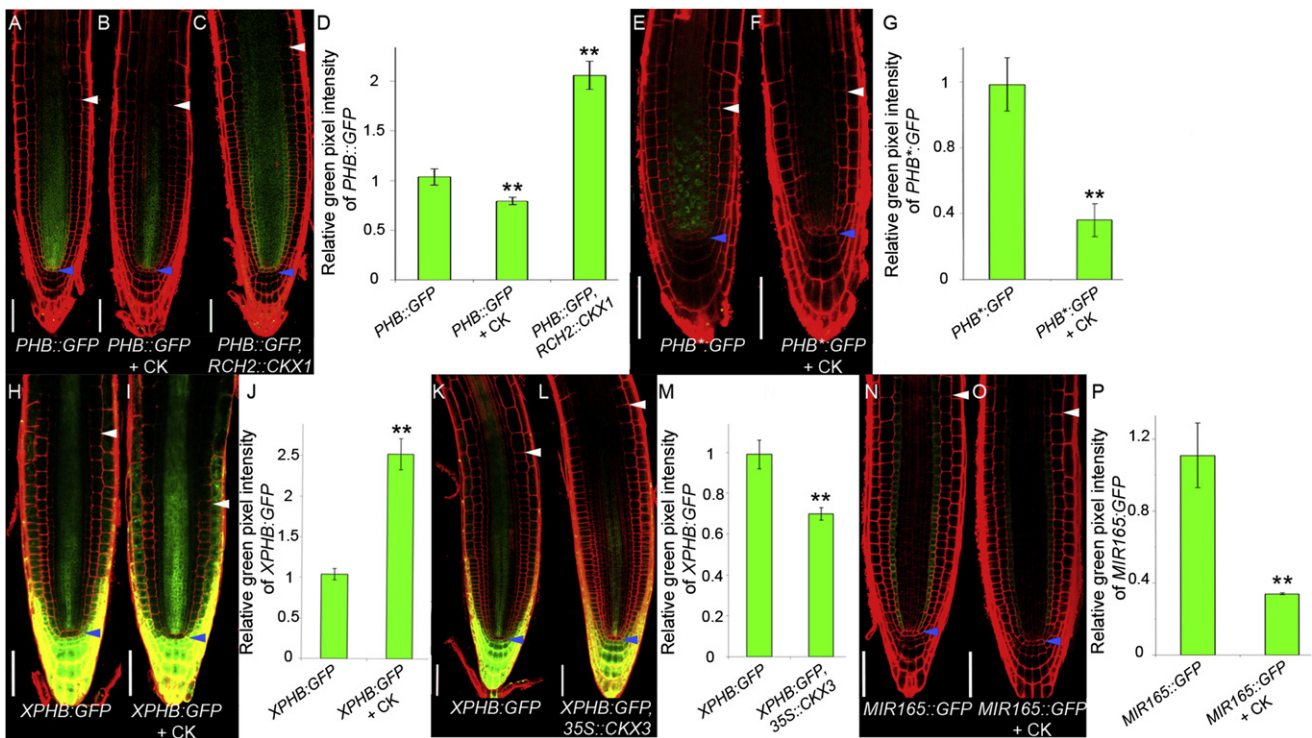
Figure 3. CK Represses Both *PHB* and *MIR165A* Expression

(A–C) Expression of *PHB::GFP* in 5-DAG root meristems of WT (A), WT treated with CK (5 µM *trans*-zeatin for 6 hr) (B), and *RCH2::CKX1* (C).

(D) Quantification of relative PHB::GFP fluorescence in the vascular TZ (white arrowhead) of the root meristem of WT, CK-treated WT (6 hr, 5 µM *trans*-zeatin), and *RCH2::CKX1* lines shows that the GFP fluorescence intensity in the vascular TZ (white arrowhead) of CK-treated plants is reduced, whereas in *RCH2::CKX1* it is enhanced. Green pixel intensity was quantified in an area comprising three cells above and three cells below the TZ, and normalization was performed in relation to WT. Error bars represent SEM; n = 20.

(E and F) Expression of *PHB*:GFP* in 5-DAG root meristems of plants grown on control medium (E) and after CK treatment (6 hr, 5 µM *trans*-zeatin) (F).

(G) Relative quantification of GFP fluorescence in the vascular TZ of the root meristem of *PHB*:GFP* and CK-treated (6 hr, 5 µM *trans*-zeatin) *PHB*:GFP* plants. Quantification was performed as in (D). Error bars represent SEM; n = 20.

(H and I) 5-DAG root meristems of *sde1-1* plants expressing the mir165/6 activity sensor *XPHB:GFP* on control medium (H) and after 16 hr of CK treatment (5 µM *trans*-zeatin) (I).

(J) Relative quantification of GFP fluorescence in the vascular TZ of the root meristem of *XPHB:GFP* plants treated with CK (6 hr, 5 µM *trans*-zeatin). Quantification was performed as in (D). Error bars represent SEM; n = 20. Note that the *XPHB:GFP* fluorescence is enhanced in the vascular TZ of CK-treated plants, indicating reduced mir165/6 activity.

(K and L) 5-DAG root meristems of WT (K) and *35S::CKX3* (L) plants expressing the mir165/6 activity sensor *XPHB:GFP*.

(M) Relative quantification of GFP fluorescence in the vascular TZ of the root meristem of *35S::CKX3,XPHB:GFP* lines. Reduction of fluorescence indicates increased mir165/6 activity. Quantification was performed as in (D). Error bars represent SEM; n = 20.

(N and O) 5-DAG root meristems of untreated (N) and CK-treated (6 hr, 5 µM *trans*-zeatin) (O) *MIR165A::GFP* plants.

(P) Relative quantification of GFP signal in the endodermis TZ of *MIR165::GFP* versus *MIR165::GFP* treated with CK for 6 hr. Treatment with CK decreased the expression of *MIR165::GFP* at the TZ. Error bars represent SEM; n = 20.

Blue arrowheads indicate the cortex stem cell; white arrowheads indicate the cortex TZ. Scale bars represent 50 µm. *p < 0.05, **p < 0.01; Student's t test. See also Figure S3.

own biosynthesis by downregulating *IPT*s (Figure S3A) [21]. This feedback is pivotal in determining the balance between division and differentiation in the root meristem [5], but the underlying molecular mechanism remains unknown. Given that PHB directly promotes CK biosynthesis, we investigated whether elevated CK activity downregulates *PHB* and *PHV* expression, thus providing a mechanism for CK limiting its own activity. We observed that a 6 hr treatment of WT plants with exogenous CK was sufficient to reduce the accumulation of *PHB* and *PHV* transcripts (Figures S3B and S3C). CK treatment also reduced the expression of transcriptional and translational *PHB* reporter genes (*PHB::GFP* and *PHB:GFP*, respectively), as well as a translational reporter gene that is insensitive to miRNA-dependent repression (*PHB*:GFP*) (Figures 3A, 3B, 3D–3G, S3E, and S3F). Therefore, CK can

repress *PHB*, and this repression has a transcriptional component. To investigate whether repression of *PHB* by CK is mediated by ARR1, we analyzed the expression pattern of *PHB::GFP* in the root of *arr1* mutants upon CK treatment. Similar to untreated *arr1* plants, *PHB::GFP* was ectopically expressed in the meristem and TZ upon CK treatment (Figures S3G–S3I), indicating that ARR1 is necessary for CK-mediated *PHB* repression. Conversely, induction of a constitutively active ARR1 protein (*35S::ARR1ΔDDK:GR*) [5] for 4 hr was sufficient to strongly reduce *PHB* and *PHV* transcript accumulation (Figures S3B and S3C), demonstrating that ARR1 is also sufficient for CK-mediated *PHB* repression and indicating that this repression is an early response to elevated ARR1 activity. Furthermore, specific depletion of CK at the TZ (*RCH2::CKX1*) caused ectopic expression of *PHB::GFP*

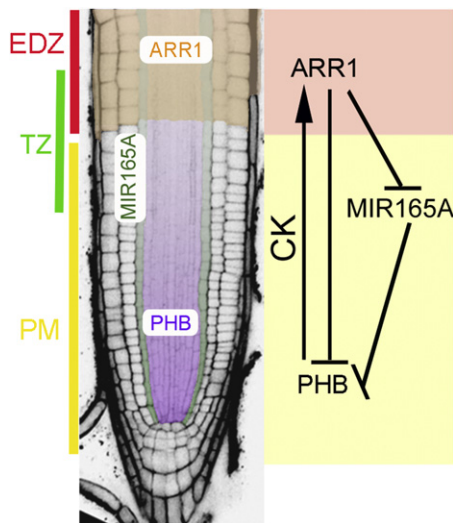**Figure 4. Model of Regulatory Interplay between *PHB*, *MIR165A*, and CK Activity**

PHB (in purple) induces CK biosynthesis in the promeristem (PM) of the root, thus activating ARR1 (in orange) in the EDZ. ARR1 represses the expression of *PHB* at the vasculature of the TZ, thus restricting *PHB* expression to the distal part of the PM. PHB expression is restricted to the vascular bundle by the activity of *MIR165A* (green) expressed in the endodermis. Notably, ARR1 also represses the transcription of *MIR165A*, thus establishing an incoherent feedforward loop. See also Figure S4.

(Figures 3C and 3D), confirming that CK prevents *PHB* expression in the TZ. Given that the short-root phenotype of *phb-1d/+* was suppressed in the *RCH2::CKX1* background (Figures 1K and 1L), we conclude that CK/ARR1-dependent *PHB* repression contributes to TZ positioning via regulating PHB-dependent CK biosynthesis.

Our observations indicate that CK can repress *PHB* expression in addition to posttranscriptional repression by miRNA165/166 (mir165/6) [8, 12, 13]. This finding raised two questions: How do these two repressive pathways relate to each other, and does a buffering mechanism maintain a basal level of PHB activity when elevated CK activity causes PHB repression? To investigate whether increased CK levels affect mir165/6-mediated regulation, we exploited a GFP transgene carrying a mir165/6 recognition sequence, which acts as a sensor of mir165/6 activity. Expression at the TZ of this mir165/6-sensitive GFP was stronger after CK treatment and weaker in CK-deficient plants (*35S::CKX3*) (Figures 3H–3M, S3J, and S3K). Consistent with these observations, CK treatment reduced the unprocessed *MIR165A* transcript levels (*priMIR165A*) and the expression of *MIR165A::GFP* in the endodermis of the TZ in WT, but not in *arr1* (Figures 3N–3P, S3D, and S3L–S3N), suggesting that CK represses *MIR165A* expression via a canonical ARR1-dependent pathway. Because PHB also promotes CK biosynthesis, these interactions give rise to a molecular circuitry wherein a signaling molecule (CK) both represses and prevents repression of a transcription factor (PHB) that in turn feeds back to promote synthesis of the signaling molecule (Figure 4). We hypothesized that this regulatory organization, termed an incoherent feedforward loop [22], might endow root development with two properties. First, it could ensure maintenance of PHB activity above a particular threshold upon rapid increase in CK activity. Second, it could allow

rapid homeostatic regulation of PHB, for example, upon fluctuations of CK that are known to occur in response to environmental changes [20, 21, 23–25]. We explored these hypotheses using computational simulations in which the dynamic response of the system to varying levels of CK activity was compared with an equivalent system in which CK did not regulate mir165/6 (Figures S4A–S4C and Computational Simulations in Supplemental Experimental Procedures). Consistent with the idea that dampening of mir165/6 by CK facilitates rapid reestablishment of PHB expression after elevation in CK activity, we observed that recovery of *MIR165A::GFP* expression after CK treatment was delayed with respect to recovery of *PHB::GFP* expression (data not shown). Our findings indicate that CK-dependent mir165/6 regulation can both dampen PHB reduction and accelerate the recovery of PHB expression in response to a temporary increase in CK. Further investigations on the effects of transient perturbations of CK activity in the context of geometric computational models of root development will help elucidate the full significance of the PHB/CK/mir165/6 incoherent loop for root growth at different developmental stages and environmental conditions.

In conclusion, we have shown how a dynamic regulatory circuitry comprising PHB and CK determines the balance of cell division and differentiation and consequently root meristem size and root length in *A. thaliana*. Notably, the transcription factor SCARECROW (SCR), which regulates root meristem size by promoting stem cell activity [26], was recently also shown to repress *PHB* expression via activating mir165 [12]. It would thus be interesting to investigate whether SCR, in addition to promoting stem cell function, also regulates root meristem size via influencing PHB-dependent CK biosynthesis. Our results, together with recent findings that CK is transported in the phloem [27], suggest that CK is synthesized in the meristem vasculature in response to PHB activity and delivered to the TZ to promote differentiation. In support of this hypothesis, the expression of *SHY2*, a CK primary target necessary and sufficient to promote cell differentiation at the TZ [5], is weaker in *phb,phv* mutants compared with WT but is reestablished after 2 hr of CK treatment (Figures S4D–S4F). Consistent with these findings, the short-root meristem phenotype of the dominant *shy2-2* mutants is suppressed in the *phb,phv* double mutant background (Figures S4G–S4K), further corroborating the idea that PHB-dependent CK biosynthesis in the distal part of the root influences cell differentiation at the proximal TZ. In addition, we have provided evidence that a PHB/CK incoherent loop allows homeostatic regulation of PHB expression upon CK perturbation. These findings provide experimental support for the suggestion, explored in recent theoretical work [28], that incoherent loops involving concurrent regulation of miRNAs and their target genes contribute to stability of gene expression programs. Thus, the mechanism we describe here may allow robust positioning of the boundary between dividing and differentiating cells upon CK fluctuations. Given that CK levels in the root are influenced by nutrient status [20, 21, 25], it will be interesting to investigate whether this mechanism also impacts on nutrient foraging in varying soil microenvironments. Furthermore, because PHB and related HD-ZIPIIIs play a pivotal role in various aspects of shoot development, including establishment of the shoot meristem and axial patterning of lateral organs [7–9, 14], it will be interesting to investigate whether the PHB/CK regulatory module identified here underpins these processes.

References

1. Dello Ioio, R., Linhares, F.S., Scacchi, E., Casamitjana-Martinez, E., Heidstra, R., Costantino, P., and Sabatini, S. (2007). Cytokinins determine *Arabidopsis* root-meristem size by controlling cell differentiation. Curr. Biol. *17*, 678–682.
2. Scacchi, E., Salinas, P., Gujas, B., Santuari, L., Krogan, N., Ragni, L., Berleth, T., and Hardtke, C.S. (2010). Spatio-temporal sequence of cross-regulatory events in root meristem growth. Proc. Natl. Acad. Sci. USA *107*, 22734–22739.
3. Blilou, I., Xu, J., Wildwater, M., Willemsen, V., Paponov, I., Friml, J., Heidstra, R., Aida, M., Palme, K., and Scheres, B. (2005). The PIN auxin efflux facilitator network controls growth and patterning in *Arabidopsis* roots. Nature *433*, 39–44.
4. Aida, M., Beis, D., Heidstra, R., Willemsen, V., Blilou, I., Galinha, C., Nussaume, L., Noh, Y.S., Amasino, R., and Scheres, B. (2004). The PLETHORA genes mediate patterning of the *Arabidopsis* root stem cell niche. Cell *119*, 109–120.
5. Dello Ioio, R., Nakamura, K., Moubayidin, L., Perilli, S., Taniguchi, M., Morita, M.T., Aoyama, T., Costantino, P., and Sabatini, S. (2008). A genetic framework for the control of cell division and differentiation in the root meristem. Science *322*, 1380–1384.
6. Moubayidin, L., Perilli, S., Dello Ioio, R., Di Mambro, R., Costantino, P., and Sabatini, S. (2010). The rate of cell differentiation controls the *Arabidopsis* root meristem growth phase. Curr. Biol. *20*, 1138–1143.
7. McConnell, J.R., and Barton, M.K. (1998). Leaf polarity and meristem formation in *Arabidopsis*. Development *125*, 2935–2942.
8. McConnell, J.R., Emery, J., Eshed, Y., Bao, N., Bowman, J., and Barton, M.K. (2001). Role of PHABULOSA and PHAVOLUTA in determining radial patterning in shoots. Nature *411*, 709–713.
9. Eshed, Y., Baum, S.F., Perea, J.V., and Bowman, J.L. (2001). Establishment of polarity in lateral organs of plants. Curr. Biol. *11*, 1251–1260.
10. Grigg, S.P., Galinha, C., Kornet, N., Canales, C., Scheres, B., and Tsiantis, M. (2009). Repression of apical homeobox genes is required for embryonic root development in *Arabidopsis*. Curr. Biol. *19*, 1485–1490.
11. Smith, Z.R., and Long, J.A. (2010). Control of *Arabidopsis* apical-basal embryo polarity by antagonistic transcription factors. Nature *464*, 423–426.
12. Carlsbecker, A., Lee, J.Y., Roberts, C.J., Dettmer, J., Lehesranta, S., Zhou, J., Lindgren, O., Moreno-Risueno, M.A., Vatén, A., Thitamadee, S., et al. (2010). Cell signalling by microRNA165/6 directs gene dose-dependent root cell fate. Nature *465*, 316–321.
13. Miyashima, S., Koi, S., Hashimoto, T., and Nakajima, K. (2011). Non-cell-autonomous microRNA165 acts in a dose-dependent manner to regulate multiple differentiation status in the *Arabidopsis* root. Development *138*, 2303–2313.
14. Prigge, M.J., Otsuga, D., Alonso, J.M., Ecker, J.R., Drews, G.N., and Clark, S.E. (2005). Class III homeodomain-leucine zipper gene family members have overlapping, antagonistic, and distinct roles in *Arabidopsis* development. Plant Cell *17*, 61–76.
15. Brandt, R., Salla-Martret, M., Bou-Torrent, J., Musielak, T., Stahl, M., Lanz, C., Ott, F., Schmid, M., Greb, T., Schwarz, M., et al. (2012). Genome-wide binding-site analysis of REVOLUTA reveals a link between leaf patterning and light-mediated growth responses. Plant J. Published online May 12, 2012.http://dx.doi.org/ 10.1111/j.1365-313X.2012.05049.x.
16. Craft, J., Samalova, M., Baroux, C., Townley, H., Martinez, A., Jepson, I., Tsiantis, M., and Moore, I. (2005). New pOp/LhG4 vectors for stringent glucocorticoid-dependent transgene expression in *Arabidopsis*. Plant J. *41*, 899–918.
17. D'Agostino, I.B., Deruère, J., and Kieber, J.J. (2000). Characterization of the response of the *Arabidopsis* response regulator gene family to cytokinin. Plant Physiol. *124*, 1706–1717.
18. Müller, B., and Sheen, J. (2008). Cytokinin and auxin interaction in root stem-cell specification during early embryogenesis. Nature *453*, 1094–1097.
19. Kakimoto, T. (2003). Biosynthesis of cytokinins. J. Plant Res. *116*, 233–239.
20. Takei, K., Ueda, N., Aoki, K., Kuromori, T., Hirayama, T., Shinozaki, K., Yamaya, T., and Sakakibara, H. (2004). AtIPT3 is a key determinant of nitrate-dependent cytokinin biosynthesis in *Arabidopsis*. Plant Cell Physiol. *45*, 1053–1062.
21. Miyawaki, K., Matsumoto-Kitano, M., and Kakimoto, T. (2004). Expression of cytokinin biosynthetic isopentenyltransferase genes in *Arabidopsis*: tissue specificity and regulation by auxin, cytokinin, and nitrate. Plant J. *37*, 128–138.
22. Alon, U. (2007). Network motifs: theory and experimental approaches. Nat. Rev. Genet. *8*, 450–461.
23. López-Juez, E., Dillon, E., Magyar, Z., Khan, S., Hazeldine, S., de Jager, S.M., Murray, J.A., Beemster, G.T., Bögre, L., and Shanahan, H. (2008). Distinct light-initiated gene expression and cell cycle programs in the shoot apex and cotyledons of *Arabidopsis*. Plant Cell *20*, 947–968.
24. Carabelli, M., Possenti, M., Sessa, G., Ciolfi, A., Sassi, M., Morelli, G., and Ruberti, I. (2007). Canopy shade causes a rapid and transient arrest in leaf development through auxin-induced cytokinin oxidase activity. Genes Dev. *21*, 1863–1868.
25. Franco-Zorrilla, J.M., Martín, A.C., Leyva, A., and Paz-Ares, J. (2005). Interaction between phosphate-starvation, sugar, and cytokinin signaling in *Arabidopsis* and the roles of cytokinin receptors CRE1/AHK4 and AHK3. Plant Physiol. *138*, 847–857.
26. Sabatini, S., Heidstra, R., Wildwater, M., and Scheres, B. (2003). SCARECROW is involved in positioning the stem cell niche in the *Arabidopsis* root meristem. Genes Dev. *17*, 354–358.
27. Bishopp, A., Lehesranta, S., Vatén, A., Help, H., El-Showk, S., Scheres, B., Helariiutta, K., Mähönen, A.P., Sakakibara, H., and Helariiutta, Y. (2011). Phloem-transported cytokinin regulates polar auxin transport and maintains vascular pattern in the root meristem. Curr. Biol. *21*, 927–932.
28. Osella, M., Bosia, C., Corá, D., and Caselle, M. (2011). The role of incoherent microRNA-mediated feedforward loops in noise buffering. PLoS Comput. Biol. *7*, e1001101.